Korean J. Chem. Eng., 32(9), 1938-1944 (2015)
DOI: 10.1007/s11814-015-0131-x

pISSN: 0256-1115
eISSN: 1975-7220

Hydrodynamic characteristics of bubbles in bubbling fluidized bed with internals

Jong-Hun Lim*, Jea-Ho Shin*, Keon Bae*, Joon-Hwan Kim, Dong-Ho Lee**, Joo-Hee Han*, and Dong Hyun Lee*,†**

*School of Chemical Engineering, Sungkyunkwan University, 2066, Seobu-ro, Jangan, Suwon, Gyeonggi-do 440-746, Korea
**Hanwha Chemical R&D Center, Korea
(*Received 4 December 2014 • accepted 16 June 2015*)

Abstract−The hydrodynamic characteristics of bubbles in bubbling fluidized beds with internals were investigated. The signal range of the optical fiber probe was calibrated from 0.5 V (the bubble phase) to 4.5 V (the emulsion phase). Data sampling involved an optical probe at a rate of 903 Hz for 725 s. To obtain improved bubble data, the data were analyzed by three processes: threshold determination, bubble analysis, and erroneous bubble elimination. The data on the bubble rise velocity and bubble frequency were measured and compared to the bed height (0.2-0.7 m), superficial gas velocity (4-7 U_{mf}), radial position r/R (0.22-0.95), number of distributor nozzles (2, 3, and 7), and the use of the internals with different hydraulic diameters of 0.19, 0.17, and 0.15 m. The experimental data were compared with several reported empirical correlations. Both the bubble rise velocity and bubble frequency increased with decreasing number of distributor nozzles. Furthermore, in the presence of internals, the bubble rise velocity decreased, whereas the bubble frequency increased with decreasing hydraulic diameter of the cross-sectional area divided by internals. Moreover, bubble breaking occurred at a specific position of r/R=0.7, not at the edge of the internals.

Keywords: Bubble Rising Velocity, Optical Probe, Internal, Bubbling Fluidized Beds

INTRODUCTION

Among many alternative energy resources with no direct carbon emission existing, the fully renewable solar energy photovoltaic industry requires a stable supply of polysilicon, which is a raw material for solar cell substrates. Bubbling fluidized bed reactors used in the synthesis of trichlorosilane (TCS, intermediate raw material of polysilicon) were used to maintain a uniform temperature distribution of the reactor, appropriate distribution of the catalytic material, and the proper contact between metal grade silicon (MG-Si), silicon tetrachloride (STC), and H_2 [1]. During this process, fluidized reactors are operated under bubbling fluidized conditions, and the gas bubbles formed by the excess exertion of gas can affect the residence time of the gas and particles, heat and mass transfer, particle entrainment, and reaction conversion. Accurate identification of the characteristics of such bubbles is a very important part of interpreting the function of fluidized beds. However, the empirical correlations established through experimental results have limits in the range of application. First, the empirical correlations made in most studies consider only temperatures below room temperature, ambient conditions, and without internal conditions. Second, even if the experiments were under the same fluidized conditions, analytical equipment, and analytical methods, the assumptions about bubble coalescence and disintegration were not similar. Therefore, to verify experimental results, comparisons are necessary between the bubble rise velocity and the empirical correlation for the bubble rise velocity made under similar experimental conditions.

Internals, the structures inside the fluidized beds, can be separated into four types: baffle, tube, packing, and inserted body. In general, their purpose is to limit the bubble size, change the hydrodynamic characteristics, adjust the particle entrainment, and improve the reaction. Glicksman et al. [2] installed horizontal tube banks inside a fluidized bed for investigating the bubble size distribution. Baffles can prevent bubbles from growing continuously, and redistribute the bubbles across the cross section of the bed. The main features of baffles are that they allow the enhancement of gas and solid heat and mass transfer, decrease in elutriation, and improvement of the radial bubble distribution [3]. According to Jiang et al. [4], Zheng et al. [5,6], and Zhu et al. [7], baffles improve the bed voidage by breaking bubbles, as well as increased mixing and contact efficiency between the gas and solid, thereby improving the reactivity.

This study was performed to investigate the effect of internals on the bubble flow in reactors producing TCS from MG-Si. The effects of vertical internals like baffles on the bubble flow characteristics were investigated in bench-scale cold fluidized bed. The bubble rise velocity was measured according to the change in the superficial gas velocity, number of distributor nozzles, and the presence or absence of internals after accurate bubble data acquired with an optical fiber probe and three bubble data processing: (1) determination of the threshold by histogram, (2) processing of the signals, and (3) bubble sorting.

EXPERIMENTAL

1. Experimental Setup

Fig. 1 shows a schematic diagram of the experimental apparatus. A gas-solid fluidized bed made of a transparent cylindrical column

†To whom correspondence should be addressed.
E-mail: dhlee@skku.edu

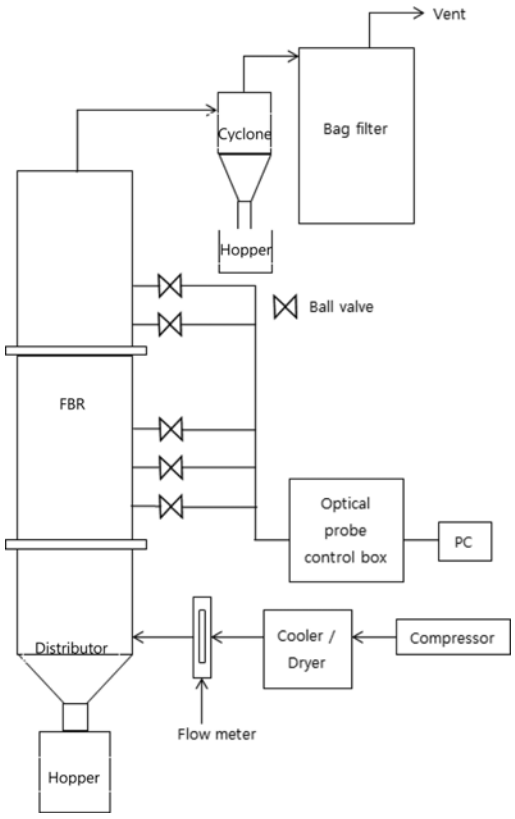

Fig. 1. Schematic diagram of experimental apparatus.

was used. The diameter and height of the cylindrical column were 0.3 and 2.4 m, respectively. The ports for the optical fiber probes were located at the column heights of 0.2, 0.3, 0.4, 0.6, and 0.7 m, because of the jet penetration and light penetration of the bed surface area. The opening fraction was determined based on ΔP_d is (0.2 to 0.4) ΔP_b [8] at U_0=0.1 m/s. The 2, 3, and 7 distributor nozzles were used, and all had opening fractions of 0.2%, determined by the following equations [9]:

$$U_{or} = C_d \sqrt{\frac{2\Delta P_d}{\rho_g}} \tag{1}$$

$$Q = N \frac{\pi d_{or}^2}{4} U_{or} \tag{2}$$

$$f_{op} = \frac{N d_{or}^2}{D_b^2} = \frac{U_o}{U_{or}} \tag{3}$$

Each distributor had a shroud nozzle installation for minimization of the particle leakage and decreased attrition between particles. More detailed specification of distributors is shown in our previous study [10].

An internal was installed for the purpose of bubble breaking and prevention of the bubble growth. The shape of the internal was a vertical baffle with a total height of 0.8 m, which is the same as used in a commercial TCS reactor. Three other types of internals were used to investigate the effect of the equivalent diameter to bubble rise velocity of the radial shape of internals (see Figs. 2(a)-(c) for the three types of internals used in this study). When internals

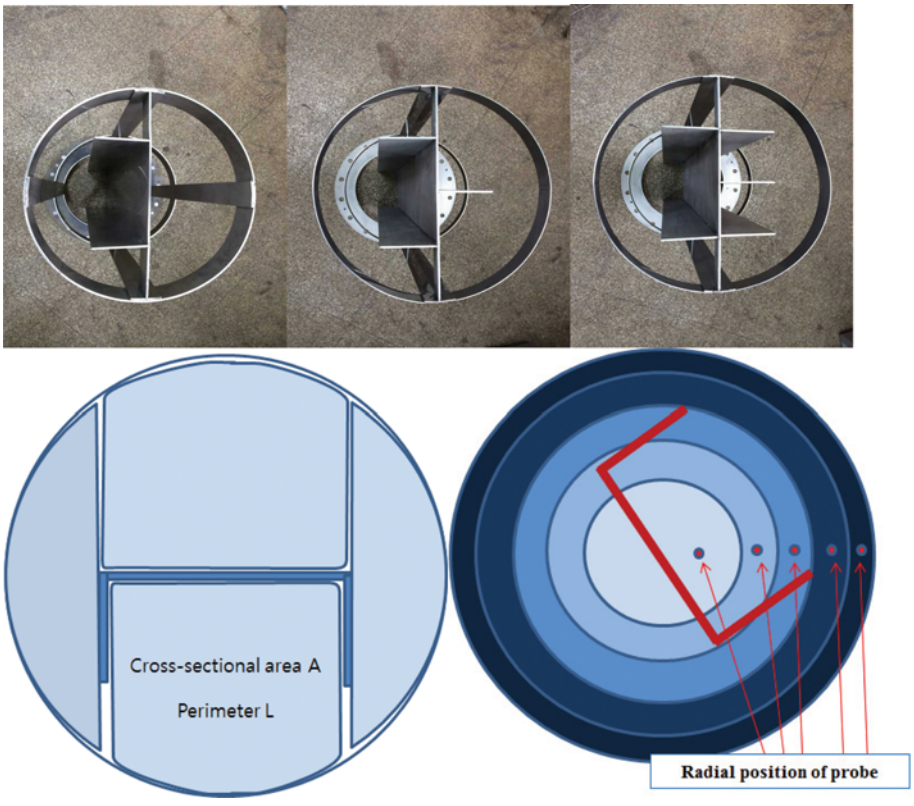

Fig. 2. Images of internals using in this study.
(a) D_{eq}=0.19 m, (b) D_{eq}=0.17 m, (c) D_{eq}=0.15 m, (d) schematic diagram of cross-sectional area, (e) radial positioning of optical probe

with various equivalent diameters were installed, the bubble flow characteristics were investigated with 2 shroud nozzle distributors.

Jet penetration length with a 2 shroud nozzle distributor was estimated by the following equations at U_o=0.1 m/s. The mean jet penetration length and maximum jet penetration were 0.14, and 0.23 m, respectively.

Knowlton et al. [11]: $$\frac{L_j}{d_{or}} = 29.7\left(\frac{U_{or}^2}{g d_{or}}\right)^{0.25}\left(\frac{\rho_g}{\rho_{bed}}\right)^{0.5}\left(\frac{d_{or}}{d_p}\right)^{0.1} \quad (4)$$

Wen et al. [12]: $$\frac{L_{j,max}}{d_{or}} = 1.3\left(\frac{U_{or}^2}{g d_p}\right)^{0.38}\left(\frac{d_{or} U_{or} \rho_g}{\mu}\right)^{0.13}\left(\frac{\rho_g}{\rho_s}\right)^{0.58}\left(\frac{d_{or}}{d_p}\right)^{0.25} \quad (5)$$

An internal was installed higher than jet penetration length to avoid the effect of jet penetration. Each internal was installed in the fluidized bed 0.45 m above the distributor. Internals with the equivalent diameters of 0.19, 0.17, and 0.15 m were designed by using the following equation:

$$D_{eq} = \frac{4A}{L} \quad (6)$$

where A and L are the mean cross-sectional area and wetted perimeter of the cell divided by internal, respectively. Fig. 2(d) shows the cross-sectional area and perimeter. Fig. 2(e) shows the radial positioning of the optical probe. The radial bed cross section was divided into five concentric circles with the same cross-sectional area. Bubble rise velocity was measured inside of the channel, which is formed by internal.

In this study, metal grade silicon (MG-Si) was used. Fig. 3 shows the particle size distribution of the MG-Si. The mean particle size (Sauter mean) determined by the sieve analysis was 149 mm, whereas the particle density and bulk density were 2,325 and 1,180 kg/m^3, respectively. The minimum fluidization velocity (U_{mf}) was experimentally measured to be 0.019 m/s. The physical properties of the MG-Si are listed in Table 1. Experimental conditions are listed in Table 2.

2. Optical Probe

The bubble rise velocity and bubble frequency were measured with an optical fiber probe prepared by the Chinese Academy of Science (Particle velocity measurer PV-6, Institute of Process Engineering). The optical fiber probe was composed of a bottom tip of channel 1 and an upper tip of channel 2 as a dual optical probe. Optical signals measured by each tip were converted to electrical signals and saved by an analog-digital converter with 12-bit resolution. Each tip was made of a multifiber to function in the voltage range 0-5 V. In the gas phase, there are no particles, and thus the reflected light was not detected. Therefore, a minimum signal is the output for the gas phase. When the particle volume phase is increased, the increase in the light reflection was observed, causing an increase in the detected light. Therefore, signal output is increased with increasing particle volume fraction. However, the signal output is not proportional to the particle volume fraction, because of the scattering of light by particles. Therefore, the bubble and emulsion phases can be distinctly identified by a threshold--the boundary signal between the gas phase and the emulsion phase. For measurements, signal output was calibrated in the range of 0.5 V (gas phase) to 4.5 V (specular reflection) using a mirror in a dark room. The thickness of each tip was 1 mm, and the tip distance was 2.13 mm. Data sampling rate was set to 1,000 Hz, and 128×2^{10} (131,072) data were sampled in a data set. Five data sets were sampled, and total sampled data numbers were 640×2^{10} (655,360). Actual sampling rate was 903 Hz, and the total sampling time was 725 s.

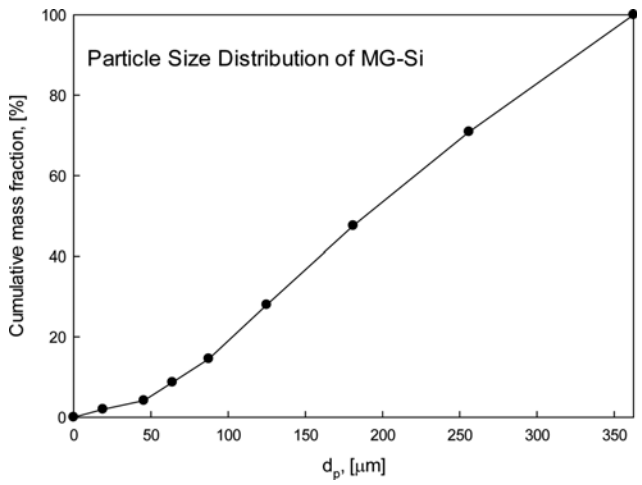

Fig. 3. Particle size distribution of MG-Si.

Table 1. Physical properties of bed material

Material	Metal grade silicon
Bulk density	1180.5 kg/m^3
Mean diameter	148.9 μm
Particle density	2325.1 kg/m^3
U_{mf}	1.9×10^{-2} m/s
ε_{mf}	0.47
Geldart classification	Group B
Shape	Irregular and non-spherical

Table 2. Experimental conditions

Fluidizing gas	Air
U_o	0.08-0.14 m/s (4-7 U_{mf})
Temperature	Room temperature
Pressure	Atmospheric pressure
Radial measuring position	r/R=0.22-0.95 (5 positions)
Experiments without internal	Distributor with 2, 3, 7 shroud nozzles, respectively
Experiments with internal	Distributor with 2 shroud nozzles

3. Bubble Data Analysis

Fig. 4(a) shows the voltage signal fluctuation in the range of 0-1 s when the optical probe was inserted into the fluidized beds. As shown, the voltage fluctuation appeared in the range of 0-0.6 s, because of the particle fluidization, whereas the bubble passed the probe at ~0.6-0.8 s. The voltage signal fell sharply at 0.6 s when the bubble arrived at the lower probe tip and then increased at 0.8 s when the bubble left the upper probe tip. However, the signals of the bottom and upper tip indicate that bubble seems to pass simultaneously in Fig. 4(a). Considering the distance between two tips,

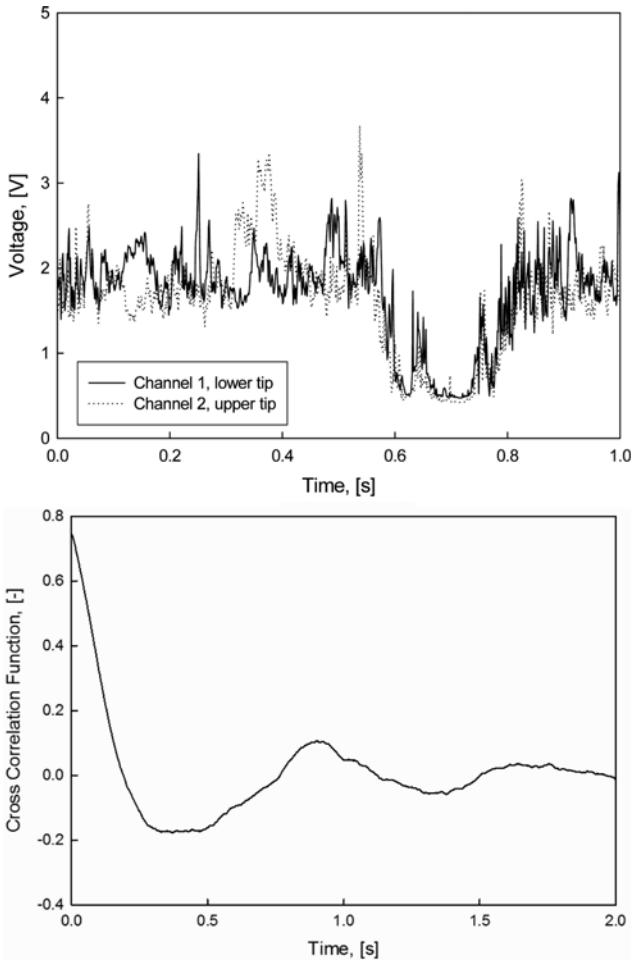

Fig. 4. (a) Measured optical probe signal in 5U_{mf} fluidized bed with 2 shroud nozzle distributors at the height of 0.7 m and r/R= 0.22. (b) Cross-correlation function of data set in Fig. 4(a).

the time of passing bubble between two tips was only a few 10^{-3} s and seems to pass simultaneously. However, specific time lag of the data in Fig. 4(a) was higher than 10^{-3} s. Because, peaks, which are not bubbles, exist, therefore specific time lag from the cross-correlation of the data in Fig. 4(a) was 0.18 s as shown in Fig. 4(b).

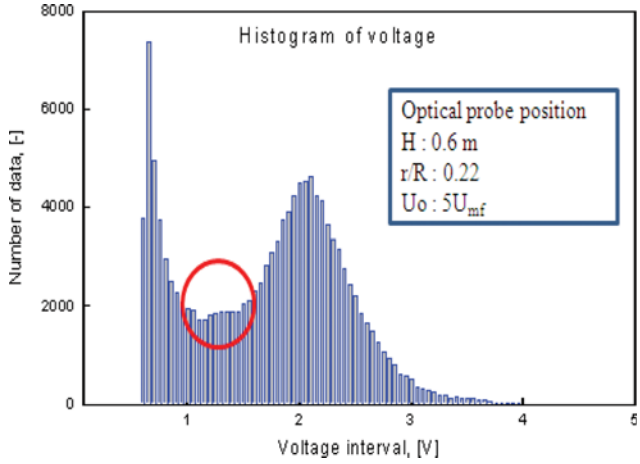

Fig. 5. Optical signal histogram in fluidized bed with 2 shroud nozzle distributors.

The voltage signals of the optical probe tips were stored in a raw data file, so data were not directly available. The threshold value to determine the bubble or emulsion state around the optical probe was needed when inserted into the fluidized beds.

Fig. 5 shows the voltage value of passing bubbles, as determined by the histogram [13]. In this figure, the maximum peak of the emulsion appeared in the range of 2-2.2 V, with a bubble maximum peak at ~0.5 V. At this time, the threshold was defined as the voltage where the tail of the histogram began, and the slope of the histogram became approximately zero. Next, the conditions were entered into the calculation program, which was programmed by MATLAB® for investigation of the bubbles using the following equations [14]:

$$T_1<T_2 \tag{7}$$

$$T_3<T_4 \tag{8}$$

$$0.7<\frac{T_3-T_1}{0.5(T_3-T_1+T_4-T_2)}<1.3 \tag{9}$$

In general, the bubble rise velocity and bubble chord length can be obtained from the following equations:

$$U_b=\frac{l_p}{T_2-T_1} \tag{10}$$

$$l_b=(T_3-T_1)\times U_b \tag{11}$$

The bubble rise velocity and bubble chord length were calculated from the raw signal data according to Eqs. (7)-(11); however, erroneous bubbles were also obtained and should be eliminated [15]. This is because all the bubbles passing an optical probe do not always rise vertically. Some bubbles pass aside the optical probe by zigzag motion, affecting the bubble chord length. The chord length measurements smaller than the distance between the probe tips were considered inaccurate. Moreover, the chord lengths larger than the bed radius were considered outliers, and the bubble rise velocity measurements >1 m/s were also rejected.

4. Empirical Correlations of the Bubble Rise Velocity

Karimipour and Pugsley [16] compared and suggested suitable empirical equations for estimation of the bubble rise velocity and bubble size. Those equations havesome correlations suitable for this study. Davison and Harrison [17] suggested the correlations of Eqs. (12), (13) for the relationship between the bubble rise velocity and bubble diameter.

$$U_{br}=0.71\sqrt{gd_b} \tag{12}$$

$$U_b=U_{br}+(U_o-U_{mf}) \tag{13}$$

Empirical correlations about bubble diameter with a bed height suitable for this study are shown by the following equations:

Darton et al. [18]: $$d_b=0.54g^{-0.2}(U_o-U_{mf})^{0.4}(h+4A_0^{0.5})^{0.8} \tag{14}$$

Mori and Wen [19]: $$\frac{d_{bm}-d_b}{d_{bm}-d_0}=\exp(-0.3h/D),\ d_{bm}=1.87d_0 \tag{15}$$

Cai et al. [20]: $$d_b=0.138h^{0.8}(U_o-U_{mf})^{0.42}\exp(-2.5\times10^{-5}(U_o-U_{mf})^2-10^{-3}(U_o-U_{mf})) \tag{16}$$

Bubble rise velocity was predicted by the above empirical correlations about bubble diameter by the correlation of Davidson and Harrison [17], and the most suitable equation was determined by comparing with experimental data.

RESULTS AND DISCUSSION

1. Effect of Number of Distributor Nozzles

The variation in the bubble rise velocity with superficial gas velocity at the heights of 0.4 and 0.7 m without jetting and dead zones is shown in Fig. 6. In Fig. 6, each point is the average of five data sets. The relative standard deviation of a whole point was 11.4%. As shown in the figure, the bubble rise velocity decreased with increasing number of shroud nozzles at a height of 0.4 m. The opening fraction of each distributor was similar; however, the nozzle diameter increased (0.005, 0.008, 0.01 m) with decreasing number of distributor nozzles (7, 3, and 2). Finally, the bubble rise velocity increased with increasing initial bubble size and decreased with increasing distributor nozzle diameter at a height of 0.7 m; however, the difference between 2 and 3 distributor nozzles was insignificant. When 2 and 3 shroud nozzle distributors were used, the initial bubble size was larger than for 7 distributors. Therefore, the rising velocity of large bubbles became similar in the upper fluidized beds, because of the bubble coalescence with increasing bed height.

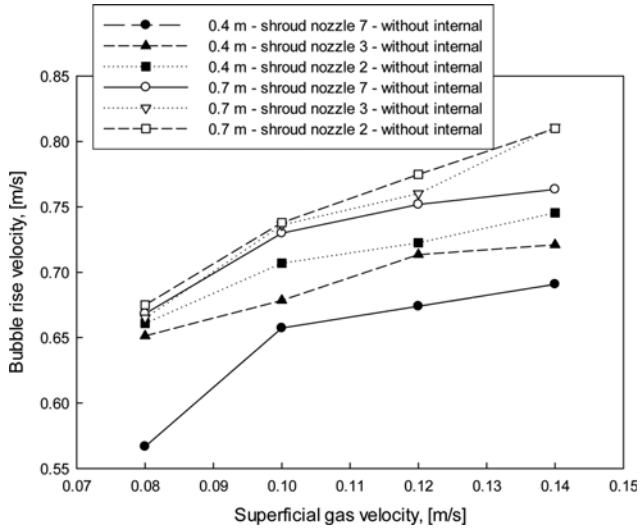

Fig. 6. Variation of average bubble rise velocity (U_b) with superficial gas velocity (U_o) according to number of shroud nozzles (2, 3, 7) at the heights of 0.4 and 0.7 m.

2. Effect of Internals

Fig. 7 shows the variation in the bubble rise velocity according to the superficial gas velocity with 2 shroud nozzle distributors, with and without internals. Because of the bubble breaking as a result of the internal, the bubble rise velocity was smaller with the inclusion of the internal than without it. With the inclusion of internals, the bubble rise velocity decreased by 7% for D_{eq}=0.19 m, 10% for D_{eq}=0.17 m, and 14% for D_{eq}=0.15 m as compared without internal. Continuous decrease in the bubble rise velocity was observed with decreasing hydraulic diameter of the internals. Calculating the gradient of the bubble rise velocity according to superficial gas velocity from Fig. 7, bubble rise velocity was faster without the inclusion of the internals by 1.44 times compared to the internal with D_{eq}=0.19 m, 1.60 times to D_{eq}=0.17 m, and 3.00 times to D_{eq}=0.15 m. As shown in Eqs. (14)-(16), bubble diameter was affected by bed diameter and cross-sectional area. Bubble diameter decreased with decreasing equivalent diameter of the channel by internal, thus decreasing bubble rise velocity with decreasing bubble diameter, as shown in the correlation by Davidson and Harrison [17]. Therefore, decreasing equivalent diameter of channel by changing positioning of baffles is effective in decreasing bubble rise velocity as shown in Fig. 7.

The bubble rise velocity according to the hydraulic diameter of the internal is shown in Fig. 8. As explained above, the bubble rise velocity decreased with decreasing hydraulic diameter of the internal, because of the bubble breaking. More specifically, the rate of the bubble rise velocity increased more with increasing hydraulic

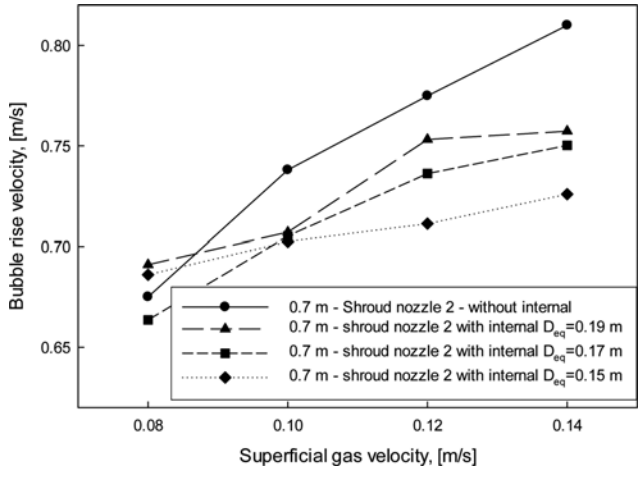

Fig. 7. Variation of average bubble rise velocity (U_b) with superficial gas velocity (U_o) for 2 shroud nozzle distributors, with and without internals.

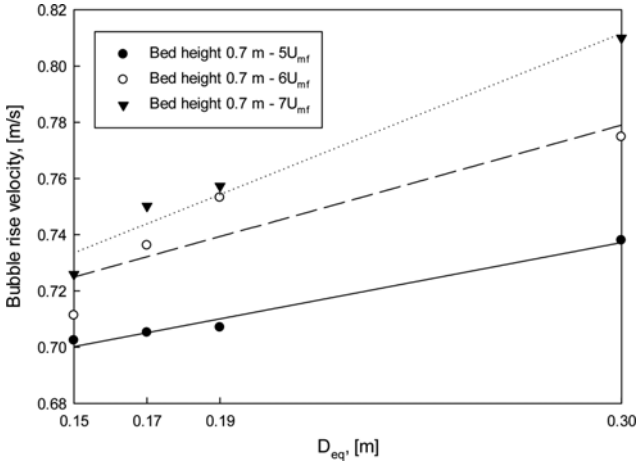

Fig. 8. Variation in bubble rise velocity with hydraulic diameter for 2 shroud nozzle distributors at the bed height of 0.7 m.

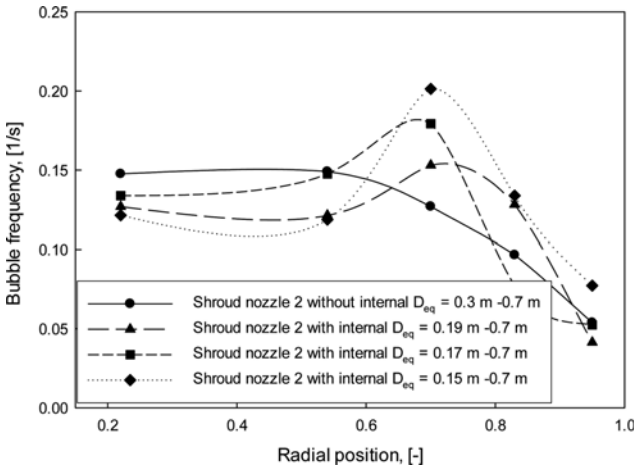

Fig. 9. Variation of bubble frequency with radial position for 2 shroud nozzle distributors, with and without internals, at U_o=0.10 m/s.

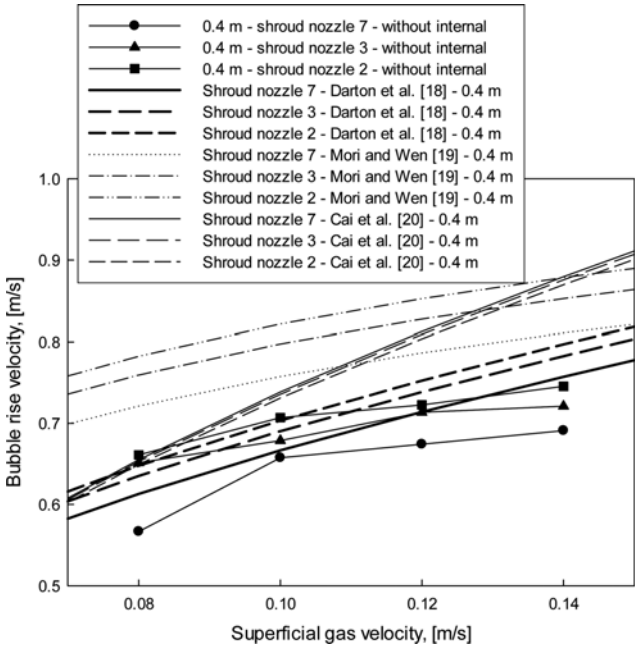

Fig. 10. Comparison between empirical correlations and experimental data.

diameter and superficial gas velocity, indicating that the effect of superficial gas velocity on the bubbles decreased in the presence of the internals and decreased with the hydraulic diameter of the column.

Fig. 9 shows the bubble frequency at the radial position (r/R) and the superficial gas velocity of 0.1 m/s. In the presence of the internals, the bubble breaking phenomenon occurred specifically at a r/R of 0.7, not at the overall edge of the internal. This result shows that bubble frequency increased with decreasing bubble size by dispersion of the bubble by the internal. The bubble dispersion effect was especially remarkable on the radial position, which shared with the shroud nozzle. Furthermore, the bubble frequency increased with decreasing hydraulic diameter in the presence of the internal. From this result, the increase in the bubble dispersion efficiency with decreasing hydraulic diameter is verified. Moreover, bubble rise velocity decreased with increasing bubble dispersion efficiency as shown in Fig. 7.

3. Comparison between Experimental Data and Empirical Correlations

The experimental data were compared to the empirical-correlation studies for the validation of the experimental bubble rise velocity. According to Kaimipour and Pugsley [16], when Geldart B particles were used, the predicted bubble size of Darton et al. [18] was more similar to the experimental data than other empirical correlations. The equation for calculating the bubble rise velocity was identified as similar to Davidson and Harrison [17], who calculated the square difference. In this study, the gas distributors had the same opening fraction but different hole sizes. The initial bubble size was an important factor for the calculation of the bubble size and rise velocity. Therefore, empirical correlations including the initial bubble size were selected for the calculation of the bubble rise velocity.

The tendency of the experimental results shown in Fig. 9 is similar to the combination by Mori and Wen [19] with Davidson and Harrison [17] in the range of 20%. Moreover, Fig. 10 shows that the empirical correlation by Darton et al. [18] combined with the study of Davidson and Harrion [17] was more similar than the correlations of other studies, coming to within 10% of the experimental data obtained herein.

CONCLUSIONS

The bubble rise velocity increased with decreasing number of distributor nozzles at similar opening fractions and decreased with decreasing hydraulic diameter of the internal. The rate of increase in the bubble rise velocity decreased continuously in the presence of the internals with decreasing hydraulic diameter. The bubble breaking phenomenon occurred specifically at an r/R of 0.7, not at the overall edge of the internal. Furthermore, the bubble frequency increased with decreasing hydraulic diameter in the presence of the internal. Overall, the predicted values by Darton et al. [18] were found to be more similar to the experimental data than other empirical correlations. The effect of the internals on the bubble rise velocity was investigated and could be useful for the design of internals with effective bubble dispersion. Bubble dispersion affects the product yield in the operation of the fluidized bed. Therefore, this study may contribute to increase the efficiency of TCS reactor.

ACKNOWLEDGEMENTS

This study was supported by the Ministry of Knowledge Economy (MKE), the Korean Institute for Advancement of Technology (KIAT), and the Honam Institute for Regional Program Evaluation (HIRPE) by the Leading Industry Development for Economic Region. This study was also supported by the R&D Center for Valuable Recycling (Global-Top R&D Program) of the Ministry of Environment with a project number of GT-14-C-01-038-0. This work was conducted under the framework of the Research and Development Program of the Korea Institute of Energy Research (KIER) (B4-2411).

NOMENCLATURE

A : cross-sectional area [m^2]
d_b : bubble diameter [m]
d_{bm} : maximum bubble diameter [m]
d_0 : initial bubble diameter [m]
d_{or} : orifice diameter [m]
d_p : particle size [m]
C_d : drag coefficient [-]
D_b : bed diameter [m]
D_{eq} : equivalent diameter [m]
f_{op} : opening fraction [-]
g : gravitational acceleration [m/s^2]
h : axial bed height [m]
L : wetted perimeter [m]
L_j : jet penetration length [m]
l_b : bubble chord length [m]
l_p : tip distance between lower and upper tip for optical fiber probe
N : nozzle number on distributor [-]
ΔP_d : pressure drop across distributor [Pa]
Q : volumetric flow rate [m^3/s]
R : column radius [m]
r : radial position [m]
T_1 : lower tip time which a bubble hit the probe [s]
T_2 : upper tip time which a bubble hit the probe [s]
T_3 : lower tip time which a bubble left the probe [s]
T_4 : upper tip time which a bubble left the probe [s]
U_0 : superficial gas velocity [m/s]
U_{or} : orifice gas velocity [m/s]
U_b : bubble rising velocity [m/s]
U_{br} : single bubble rising velocity [m/s]
U_{mf} : minimum fluidization velocity [m/s]

Greek Letters

ρ : density [kg/m^3]
μ : viscosity [kg/m·s]

Subscripts

g : gas
p : particle
s : solid

REFERENCES

1. J. H. Han, *News & Information for Chemical Engineers*, **31**, 313 (2013).
2. L. R. Glicksman, W. K. Lord, M. Sakagami, *Chem. Eng. Sci.*, **42**, 479 (1987).
3. Y. Jin, F. Wei and Y. Wang, Effect of Internal Tubes and Baffles, *Handbook of Fluidization and Fluid-Particle Systems*, Ed. by Yang, W. C., Marcel Dekker, Inc., New York (2003).
4. P. Jiang, H. T. Bi, R. H. Jean and L. S. Fan, *AIChE J.*, **37**, 1392 (1991).
5. C. G. Zheng, Y. K. Tung, Y. S. Xia, B. Hun and M. Kwauk, Voidage redistribution by ring internals in fast fluidizationm, *Fluidization '91*, 168 (1991).
6. C. G. Zheng, Y. K. Tung, H. Z. Li and M. Kwauk, Characteristics of fast fluidized beds with internals, *Fluidization VII*, 275 (1992).
7. J. X. Zhu, M. Salah and Y. M. Zhou, *J. Chem. Eng. Jpn.*, **30**, 928 (1997).
8. Karri SBR, PSRI Research Report No. 60 (1990).
9. Karri SBR, Grid Design Chapter, PSRI Design Manual (1991).
10. J. H. Lim, Y. Lee, J. H. Shin, K. Bae, J. H. Han and D. H. Lee, *Powder Technol.*, **266**, 312 (2014).
11. T. Knowlton, R. Karri and R. Cocco, PSRI Fluidization Seminar and Workshop, Particulate Solid Research Inc. (2011).
12. C. Y. Wen, N. R. Deole and L. H. Chen, *Powder Technol.*, **31**, 175 (1982).
13. J. M. Schweitzer, J. Bayle and T. Gauthier, *Chem. Eng. Sci.*, **56**, 1103 (2001).
14. J. Zhang, Bubble columns and three-phase fluidized beds: Flow regimes and bubble characteristics, *Ph. D. Thesis, The University of British Columbia* (1996).
15. C. Sobrino, J. A. Almendros-Ibanez, D. Santana, C. Vazquez and M. de Vega, *Chem. Eng. Sci.*, **64**, 2307 (2009).
16. S. Karimipour and T. Pugsley, *Powder Technol.*, **205**, 1 (2011).
17. J. F. Davidson and D. Harrison, Fluidized particles, *Cambridge University Press*, London (1963).
18. R. C. Darton, R. D. La Naueza, J. F. Davidson and D. Harrison, *Trans. Inst. Chem. Eng.*, **55**, 274 (1977).
19. S. Mori and C. Y. Wen, *AIChE J.*, **21**, 109 (1975).
20. P. Cai, M. Schiavetti, G. D. Michele and G. C. Grazzini, *Powder Technol.*, **80**, 99 (1994).